EFFECT OF THE BORIDING SURFACE-HARDENING PROCESS OF AISI 304L ON THE VIABILITY OF HFOB CELLS

Enrique Hernández-Sánchez[1]*, Nadia Ivette Godínez-Zamora[1], Ángel Ernesto Bañuelos-Hernández[2], Nury Pérez-Hernández[2], Raúl Tadeo-Rosas[3], Luz Alejandra Linares-Duarte[1], Yesenia Sánchez-Fuentes[1]

[1]Instituto Politécnico Nacional, Unidad Profesional Interdisciplinaria de Biotecnología, Departamento de Bioingeniería Avenida Acueducto s/n Barrio La Laguna Ticomán, México City 07340, México.

[2]Instituto Politécnico Nacional, ENMH, Laboratorio de Microbiología, Av. Guillermo Massieu Helguera 239, La Escalera, México City 07320, México.

[3]Facultad de Ingeniería Mecánica y Eléctrica, Universidad Autónoma de Coahuila, Unidad Torreón, Carretera Torreón-Matamoros, km 7.5, Ciudad Universitaria, Ejido el Águila, Torreón Coahuila 27276, México.

Abstract

AISI 304L stainless steel is an austenitic steel with general uses. However, its chemical composition and mechanical properties are relatively similar to those of AISI 316L. The main difference between the two steels is probably the molybdenum content in AISI 316L, which makes it more apt to face corrosion. This study evaluates the possibility of offering AISI 304L as an alternative to the demand for materials resistant to corrosion in biomedical applications by improving its chemical and mechanical surface properties. First, samples of AISI 304L were thermochemically treated with a thermochemical hardening process known as boriding to generate a hard surface layer of iron borides, the FeB/Fe_2B type, on the steel samples. The boriding process has been demonstrated to be effective in protecting the surface of treated materials against wear and corrosion, even in chloride-rich environments. The thermochemical powder-pack boriding process was performed at a constant temperature of 950 °C for 2, 4, and 6h. The effect of the hard layers on the cellular viability of human fetal osteoblast (HFOb) cells was evaluated using a resazurin reduction (CellTiter Blue) assay. After 2, 4, and 6h of exposure to the treatments, layers of FeB/Fe_2B with 12.30, 23.60, and 30.65 µm thicknesses were obtained, respectively. The hardness of the layers ranged from 1992.40 to 2397.54 HV (at least ten times higher than that of the non-treated steel). The viability results suggest that the samples exposed to boriding exhibited better cellular proliferation than the non-treated AISI 304L steel. These results open the possibility of generating materials with better capability to face corrosion and wear conditions in biological environments.

Keywords: *boriding process, hard layers, biomaterials, biocompatibility, corrosion resistance*

1. INTRODUCTION

The use of some metals, such as titanium alloys, cobalt alloys, and stainless steel, in orthopedic applications has been highly favored in recent decades. The main reason for their use is their excellent mechanical properties and great corrosion resistance. Nevertheless, although these metals are specially designed to address corrosion, the damage caused by corrosion has not been totally controlled, especially when in contact with bodily fluids [1]. In the case of biomedical steel, AISI 316L stainless steel is widely used in the biomedical industry, mainly in biomedical implants, due to its corrosion resistance, making it a low-cost, biocompatible option. On one hand, the low carbon content of AISI 316L does not cause intercrystalline corrosion. On the other hand, this type of steel may corrode the inside of a human body under certain conditions [2]. Different surface modification processes have been presented as alternatives to minimize the corrosion of AISI 316L steel when it is in contact with living tissue [3]. Under this context, one of the most recently used processes to modify the surface of metallic materials is boriding, consisting of diffusing boron atoms into the metallic matrix to enhance its mechanical and chemical surface properties. The process takes place in solid, liquid, or gaseous media. The most

commonly used method is powder-pack boriding because it is cheaper and easier to perform than the other methods. Several researchers have reported improvements in the surface properties of AISI 316L SS using the boriding process. For example, Himanshu Balhara and co-workers [4] exposed AISI 316L to a novel process of boriding called "direct energy deposition." They obtained flat layers composed mainly of FeB and Fe_2B with a 20 µm thickness and a 2000 HV hardness. M.Y. García-Santibañez and co-workers [5] reported an improvement in the wear resistance of AISI 316L following powder-pack boriding. They reported layers with a 28 µm thickness, composed mainly of a biphasic layer of FeB/Fe_2B. Likewise, R.A. García-León [6] exposed AISI 316L to a powder-pack boriding process to form a hard surface layer on the AISI 316L SS. The researchers reported biphasic layers of FeB/Fe_2B with a 39 µm total length and between 21 and 23 GPa hardness for the FeB phase.

Many researchers have focused on improving the surface properties of AISI 316L SS by applying the thermochemical boriding process. Nevertheless, the presence of molybdenum (Mo) in the alloying elements of AISI 316L SS represents a complication during the manufacturing process. Under this context, austenitic AISI 304L SS exposed to the boriding process appears to be a possible substitute for the AISI 316L SS in areas where surface resistance to wear and corrosion is very important. AISI 304L SS is the most commonly used SS due to its exceptional resistance to corrosion, low cost, and outstanding mechanical characteristics [7]. Nonetheless, many researchers have focused on improving the surface properties of AISI 304L SS and AISI 316L by means of the thermochemical boriding process, even though these two steels share practically the same chemical composition. In fact, the only difference is the Mo content in AISI 316L, but as has been mentioned above, Mo does not appear to be a relevant component in the resulting hard layers.

In this research, the surface properties of AISI 304L steel were improved following boriding to explore the possibility of transforming a commonly used steel into a steel with superior surface properties. The chemical composition of the resulting layers was analyzed with X-ray diffraction, and their physical and mechanical properties were analyzed and compared with those reported in the literature for AISI 316L. Furthermore, the cellular viability of HFOb cells on the modified surfaces was evaluated to offer an alternative high-quality, low-cost material for medical applications.

2. MATERIALS AND METHODS

2.1. Materials

The materials used to develop the present research work are summarized in Table 1.

Table 1. Materials used for the development of the experimental procedure.

Procedure	Material	Description
Thermochemical process	AISI 304L stainless steel	An AISI 304L stainless steel bar 20 mm in diameter and 300 mm in length
	Distilled water	Impurity-free water for sample cleaning
	Ethanol	Reagent for sample cleaning
	SiC sandpaper	Abrasive paper for roughing up the samples
	Alumina (0.05µm)	Abrasive powder for mirror-finishing the samples
	Durborid G	Boron mixture with 90% wt. SiC, 5% wt. B_4C, and 5% wt. HBF_4K
	Cryovials	Cell storage container
	Centrifuge tubes	Container for centrifugating the cellular liquids

Biological tests	Pipettors	Tools used for fluid handling
	Test tubes	
	T75 bottle	Tool used for cellular culture
Cell culture	HFOb cells	

2.2. Methods

2.2.1 Sample preparation

Cylindrical samples 20 mm in diameter and 4 mm in length were cut from a cylindrical AISI 304L stainless steel bar. Table 2 depicts the chemical composition of the 304L SS.

Table 2. Chemical composition of the AISI 304L stainless steel.

Element	**C**	**Mn**	**Ni**	**Cr**	**Si**	**P**	**S**	**Fe**
%w.	0.03	2.00	8.25-12.50	18.00	1.01	>0.05	>0.03	Balance

The samples were prepared following a metallographic process, consisting of grinding them with a sequential series of SiC abrasive papers of different meshes (100, 220, 320, 400, 600, and 1000).

After the metallographic process, the samples were sonicated for 5 min in a mixture of ethanol and distilled water (50/50) to eliminate grease and impurities.

2.2.2 Boriding process

After the metallographic process, the samples were introduced into a 304 stainless steel crucible containing the boron powder source (DURFERRIT, G) and covered up to 15 mm on each side to prevent oxidation during the boriding process and to ensure the best results [3] thus. In accordance with previous works [8,9], the treatment temperature remained constant at 950 °C because that temperature achieves the best results in terms of the quality of the layers [10,11,12]. The treatment time was established as 2, 4, and 6 h.

2.2.3 Surface characterization

Once the boriding concluded, the furnace was turned off, and the samples were cooled to room temperature inside the furnace. The samples were then rinsed in an ultrasonic bath for 10 min in 50/50 ethanol/water to remove any remaining boride impurities.

The samples were then cross-sectioned and prepared for microscopic examination following standard metallographic techniques. The boride layer thicknesses were measured via optical microscopy with a GX-51 optical microscope (Olympus, Center Valley, PA, USA). At least 100 measurements were obtained in different zones of the layers to obtain a mean value of the layer thickness. The morphology and nature of the boride layers were determined via scanning electron microscopy (SEM) (JSM-6360LV, JEOL, JEOL Ltd., Akishima, Japan), using 20 kV of energy. The nature and crystalline structure of the boride layers were analyzed via X-ray diffraction (XRD) using a D8 FOCUS diffractometer (Bruker, Billerica, MA, USA) equipped with Cu-K radiation (1.5418 Å).

2.2.4 Mechanical characterization

The hardness of the boride layers was measured using a microhardness tester (CMS Metrology, Tlalnepantla de Baz, Mexico), according to the guidelines of the ASTM E384 standard [13]. A constant load of 0.025 kg was applied in the middle of the boride layer.

To obtain a mean value for the layer hardness, at least ten indentations were performed. The indentations were spaced at least 2.5 dV apart (Vickers diagonal) to avoid interactions with each other [13].

2.2.5 Cellular interaction

All of the tests related to the cellular culture were performed in the Osteoarticular Diseases Laboratory of the Escuela Nacional de Medicina y Homeopatía (ENM y H) of the Instituto Politécnico Nacional (IPN), México. The tests were conducted in accordance with the laboratory's biosecurity levels (BSLs).

2.3.1 Defrosting and cellular activation

Before the tests began, the HFOb cells were frozen in a special container between -190 and -195 °C to preserve their viability and functionality [14]. When the tests began, the cells were defrosted with the aid of body temperature, as shown in Fig. 1. It is important to note that the cells must be defrosted as fast as possible to the ideal temperature (35-37 °C) to avoid damaging any of the cellular membranes due to crystal formation [15].

Fig. 1. Defrosting technique for cellular activation: (a) cryogenic vial and (b) use of body temperature for defrosting the cells.

The specifications for handling the HFOb cell line are presented in Table 3.

Table 3. Specifications for handling the HFOb cell line during the cellular culture assays.

Cellular line	Human fetal osteoblast (HFOb) cell line ATCC CRL11372
Culture medium	Dulbecco's Modified Eagle's Medium
Culture medium supplement	DMN and Ham´s F12 supplemented with 10% FBS and routine antibiotics
Speed and time of centrifugation	140 G (rcf), 26 °C, 5min.
Incubation conditions	37 °C, CO_2 5%

2.3.2 Cell Culture of HFOb Cells

The human fetal osteoblast (HFOb) cell line ATCC CRL11372 was acquired from the American Type Culture Collection (Manassas, VA, USA). The cells were grown in Dulbecco's Modified Eagle's Medium (Gibco, Life Technologies, Paisley, UK). They were supplemented with 10% (v/v) fetal bovine serum (FBS JR Scientific, Woodland, CA, USA) and penicillin-streptomycin (Sigma-Aldrich, Toluca, Mexico). The cells were preserved at 37 °C under 5% CO_2 in a humidified incubator in the culture

medium, which was refreshed as needed. The cells were grown in traditional culture plates before they contacted the treated and non-treated steel samples. The HFOb cell line was grown at 37 °C to slow the cell growth rate. Their cellular differentiation was tested recurrently by monitoring mineralization with Von Kossa staining. The SV Tag was stable at temperatures below 40 °C, indicating that the current state of our cell line was not differentiated.

2.3.3 Proliferation Assays in HFOb Cells

The treated and non-treated samples were autoclaved (121 °C, 30 min) and placed in a 12-well polystyrene plate. Then, the wells were seeded with the HFOb cells (500 µL of a cell suspension of 10^5 cell/mL). The HFOb cells were cultured for 24 h to allow cell attachment, and the culture medium was then replaced and maintained for another 24 h.

The cellular proliferation was evaluated in two steps:

Step 1: Viability evaluation.

To determine the proliferation capacity of the HFOb cells, a resazurin reduction (RR) assay, or Alamar Blue, was used. This assay uses a dye that accepts electrons into the electron transport chain between the final reduction of oxygen and cytochrome oxidase by replacing molecular oxygen as the electron acceptor [15].

Step 2: Active viability evaluation (sample safety).

This step was performed to corroborate the safety of the treated samples in avoiding the death of the seeded cells: After 24 h of incubation, the samples were removed from the wells and cleaned twice with PBS. Then, they were placed in a new 12-well plate and incubated for another 24 h.

3. RESULTS AND DISCUSSION

3.1 Surface characterization

Fig. 2 shows cross-section micrographs of the boride layers obtained on the borided AISI 304L SS samples for the different treatment conditions. Compared with borided low-carbon steels, where the boride layers' growth is highly jagged, the morphologies of the obtained layers were flat, which is expected when SS is exposed to boriding [16,17]. The high content of alloying elements in the substrate can explain these flat morphologies of the boride layers. Specifically, Cr and Ni react with boron during the process and form compounds such as CrB, Cr_2B, NiB, and Ni_3B, which act as a diffusion barrier, consuming much of the available energy and inhibiting the growth of the boride layers. Therefore, the layer thickness in the boride stainless steel is always lower than that of low-carbon steels obtained under the same treatment conditions [16,18].

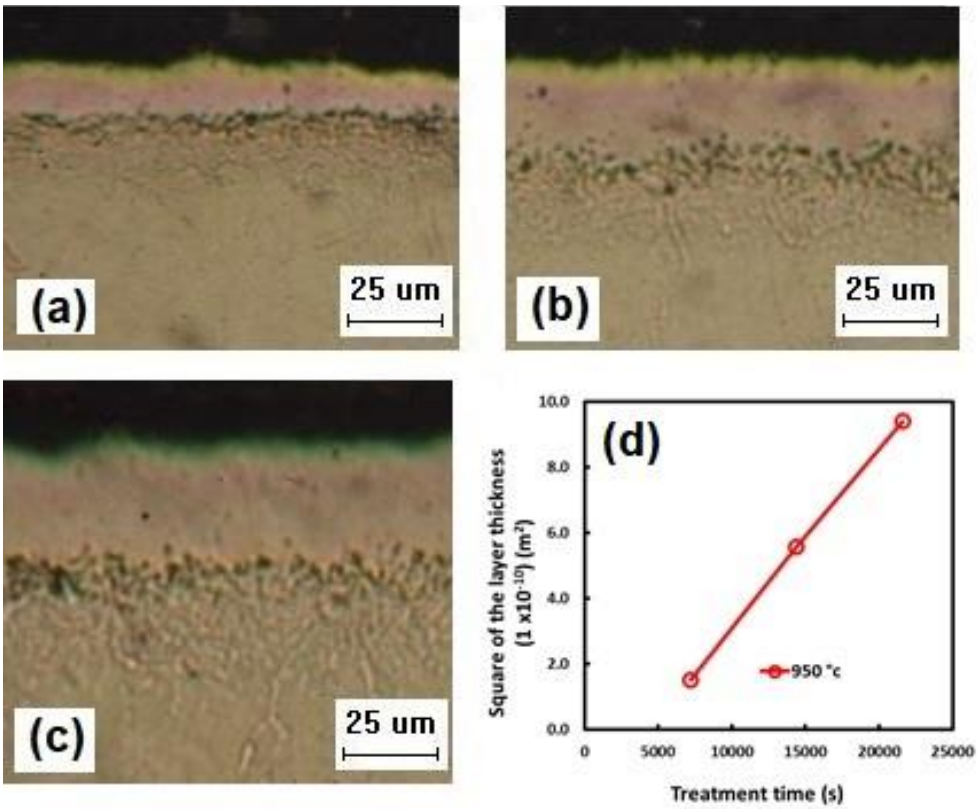

Fig. 2. Cross-section of the samples exposed to 950 °C during a) 2h, b) 4h, and c) 6h of treatment, d) is the behavior of the layer's thickness as a function of the treatment time.

Three different zones can be inferred by observing the OM micrographs of the cross-sections of the borided samples (Fig. 2). The outermost zone (zone 1), is the boride layer, which is mainly composed of a double-phase FeB/Fe_2B-type layer. Compounds such as CrB and NiB are also present but to a lower extent. A second zone (zone 2), the diffusion zone, lies below the boride layer. The third zone is the substrate (zone 3), unaffected by boron diffusion. The boride layer's morphology and chemical composition (see Fig. 2) are similar to those reported in the literature for AISI 316 SS exposed to the powder-pack boriding method [18,19].

The layer thickness ranged from 12.31 to 30.65 μm for samples exposed to 2 and 6 h, respectively. Fig. 2 shows that the increase in the layer's thickness obeys a parabolic law following Equation (1) [20]:

$$x^2 = Kt \qquad (1)$$

where x is the thickness of the boride layer (m); t is the treatment time (s); and K is the constant of parabolic growth (m^2s^{-1}), which is related to the treatment temperature and the activation energy [20,21].

As shown in Equation (1), as the treatment temperature remained constant during the process (950 °C) and the constant of parabolic growth remained steady, the boride layer thickness only depends on the treatment time, as shown in Fig. 2d.

The layer thicknesses and the constants of parabolic growth are depicted in Table 4.

Table 4. Layer thicknesses and constants of parabolic growth under different treatment conditions.

Treatment time	Layer thickness		*K*
(h)	(μm)	(m)	(m^2s^{-1})
2	12.31±1.45	$1.23x10^{-5}$	
4	23.60±2.70	$2.36x10^{-5}$	
6	30.65±2.58	$3.06x10^{-5}$	5.47×10^{-14}

The layer thicknesses and parabolic growth constants are concordant with those reported in the literature for stainless steel when exposed to boriding under similar treatment conditions [22,23]. The thickness of the layers for 304L steel was thinner than that obtained in a low-alloy steel [24,25], explained by the alloy elements acting as a barrier that hinders diffusion [16]. Therefore, the growth of these layers requires more energy than that required for low-alloyed steels [26].

The XRD analysis revealed the presence of FeB (orthorhombic) and Fe_2B (tetragonal) phases on the sample's surface, as shown in Fig. 3.

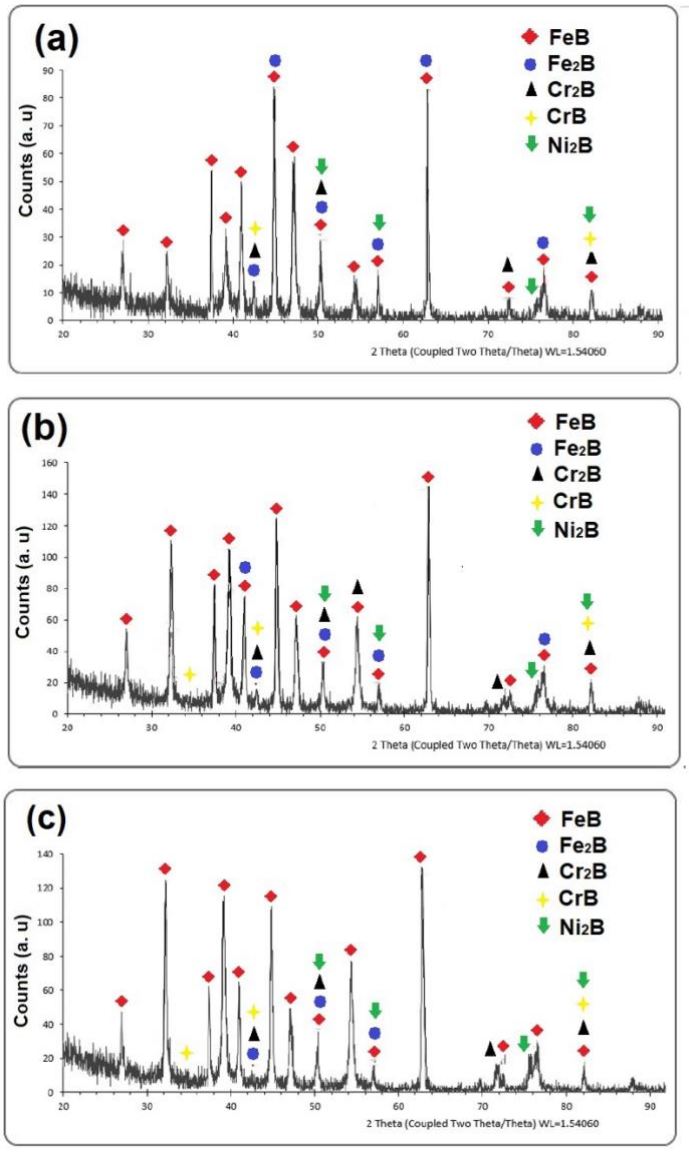

Fig. 3. X-ray patterns of the sample exposed to (a) 2 h, (b) 4 h, and (c) 6 h of treatment.

Additionally, some indications of the CrB, Cr_2B, and Ni_2B phases were observed in the RXD patterns of the treated samples. This behavior of the boride layers seen on the surface of SS agrees well with that reported in the literature, especially in the borided austenitic steels where the FeB and Fe_2B phases are the main phases and chromium and nickel borides appeared in the interphase between the diffusion zone and the boride layer [27,28]. Interestingly, the same constituents of the boride layers have been reported in the literature when AISI 316L is exposed to boriding [6,29], even when that steel contains certain amounts of Mo, indicating that the Mo content in AISI 316L does not have any influence on layer formation. These results allow us to suppose that when AISI 304L steel is exposed to a boriding treatment, its surface is modified in the same way as that of AISI 316L steel, so the boriding process can be assumed to make AISI 304L steel as biocompatible as AISI 316L steel.

3.2 Mechanical characterization

The hardness of the boride layers was measured by Vickers microindentation. To ensure correct measurements, at least five indentations were performed in the middle of the layer. Fig. 4 shows the indentations created on the sample exposed to 950 °C for 6 h.

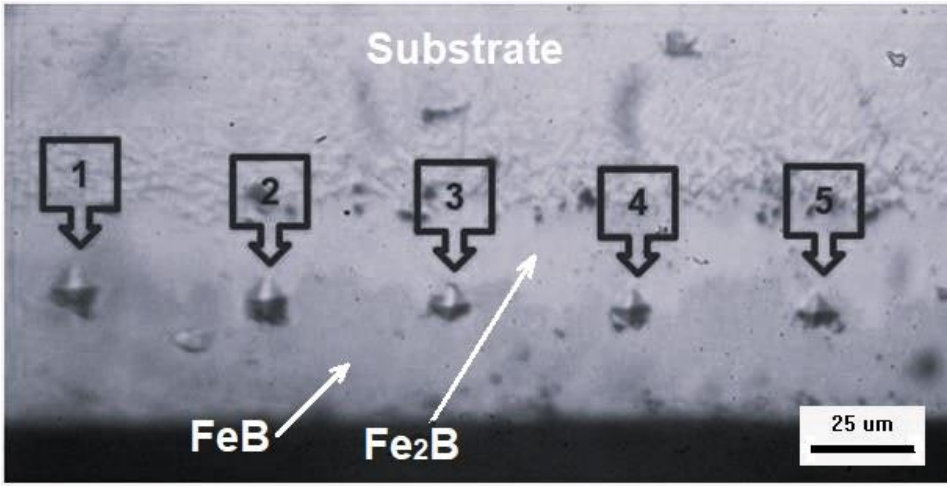

Fig. 4. Indentations created on the cross-section of the borided sample of ISI 304L.

The resulting hardness values were 195, 1942.40, 2212.16, and 2397.54 HV for the samples exposed to 0, 2, 4, and 6 h of treatment, respectively. Fig. 5 shows the hardness behavior as a function of treatment time.

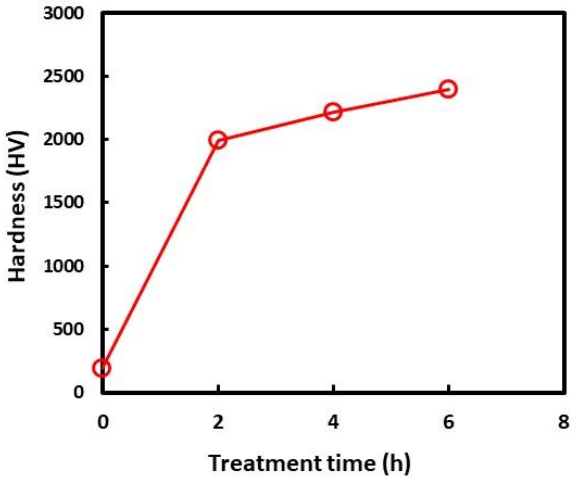

Fig. 5. Hardness behavior as a function of treatment time.

As shown in Fig. 4, the hardness of the layers is highly dependent on the treatment time. The hardness increased as the treatment time increased, explained by the boriding process being activated by the treatment conditions (time and temperature). When the boriding conditions are adequate, and the temperature for boron mobility is reached, the boride layers start to form. Then, with a constant boron flux, the layer continues to grow in a parabolic form [20], and the boron concentration in the layer also increases. Then, as the layer's thickness increases and the boron concentration increases, the resulting layer becomes more compact, and the substrate has less influence on the layer's properties. Therefore, with constant temperature, the layer´s formation only depends on the treatment time [26].

3.3 Cellular viability evaluation

Fig. 6 shows the 12-well plate with the treated and non-treated samples and the HFOb cells after 24 h of seeding (step 1).

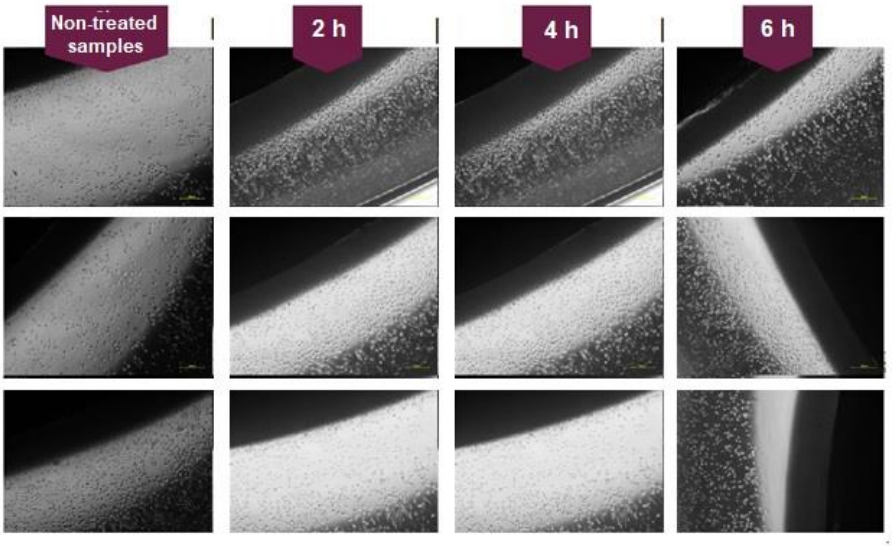

Fig. 6. Presence of the cells on the treated and non-treated samples after 24 h.

According to Fig. 6, high cell proliferation can be observed on the surface of the treated and non-treated samples after 24 h of seeding. The cellular concentration seems to be higher in the treated samples than in the non-treated samples, indicating a possible improvement in the biocompatibility of the AISI 304L steel.

The graph in Fig. 7 confirms the abovementioned results. The resazurin reduction percentage during step 1 indicated a high concentration of living cells on the treated samples, especially when exposed to 2 h of treatment.

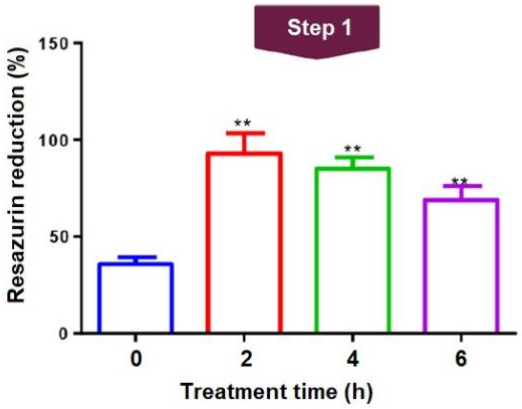

Fig. 7. Behavior of the resazurin reduction (%). ** Significant difference from the non-treated 304L SS.

Additionally, the samples exposed to 4 and 6 h of treatment exhibited lower percentages of living cells than those exposed to 2 h. In fact, by observing the graph (Fig. 7), the percentage of living cells can be assumed to be inversely proportional to treatment time. Those results let us conclude that short treatment times are better for improving the mechanical properties of AISI 304L SS without affecting the biocompatibility of the steel during the first 24 of cell exposure.

The resazurin reduction percentage during step 2 is shown in Fig. 8.

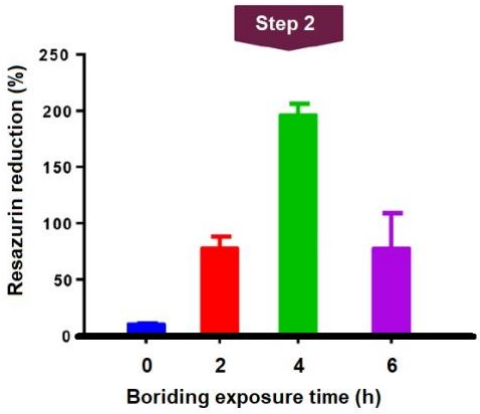

Fig. 8. Behavior of the percentage of the resazurin reduction test, step 2 (safety of the samples).

After finishing step 2 of the viability tests, some differences were observed compared with step 1 (Fig. 8). The resazurin reduction percentage in this step showed an important concentration of living HFOb cells on the samples exposed to 4 h of the boriding treatment. That behavior suggests that the cells have a period of adaptation (step 1); once that period concludes, the cells continue proliferating. The high cellular concentration in the samples exposed to 4 h of treatment is probably related to the best characteristics of the boride layer obtained in that treatment condition because the layers formed at 2 h of exposure are thinner and inconsistent, while the layers formed after 6 h of treatment were thicker but showed detachment, causing apparent cellular death. These results are consistent with those reported in the literature. For example, R. A. García-León and co-workers [6, 29] reported that boride layers formed on 316L SS after 4h of treatment. They reported compacted biphasic layers (FeB/Fe_2B type), with a 39 µm thickness and a hardness of 23 GPa (2344 HV). Additionally, they did not report the presence of Mo-borides, which is the main difference regarding the AISI 304L steel studied in this work.

4. DISCUSSION

The boriding process was successfully applied to an AISI 304L stainless steel to explore the possibility of generating a protective layer to improve not only the mechanical properties but also the chemical properties of the steel, as has been reported for AISI 316L steel. The resulting layers were mainly composed of a biphasic layer of FeB/Fe_2B with a flat morphology following growth, which is expected when SS is exposed to boriding [16,17]. The flat morphology of the boride layers can be explained by the high content of alloying elements in the substrate. Specifically, Cr and Ni react with boron during the process and form compounds such as CrB, Cr_2B, NiB, and Ni_3B, which act as a diffusion barrier that consumes much of the available energy during the process, inhibiting the growth of the boride layers. Therefore, the layer thickness of the boride stainless steel is always lower than that obtained on low-carbon steels under the same treatment conditions [16, 18].

The layer thickness ranged from 12.31 to 30.65 μm for samples exposed to 2 and 6 h, respectively. The growth of the layer's thickness obeys a parabolic law, $x^2 = Kt \quad (1)$, which is considered a particular solution to the second law of Fick [30].

Equation (1) shows that the layer's thickness depends on the treatment time and the parabolic growth constant (*K*). It involves the temperature and the boron concentration in each phase of the boriding process [30].

The thickness, crystalline structure, chemical composition, and mechanical properties of the boride layers were similar to those reported from the AISI 316L biomedical steel when exposed to boriding under the same treatment conditions [6,29]. Apparently, the presence of molybdenum in the chemical composition of AISI 316L (which is its main difference from ASI 304L steel) has no relevance in the characteristics of the resulting layers when exposed to boriding. In that sense, AISI 304L could be reasonably assumed to turn into a material suitable for biomedical applications after being exposed to the boriding process. The results of the viability tests applied to the treated samples indicated a significant improvement with respect to those shown for the non-treated samples. The best cellular response to the treated samples compared with the non-treated samples was probably due to the borided layers having better corrosion resistance than the non-treated SS, as has been established by different authors [6,28,29].

5. CONCLUSIONS

Based on the results obtained in this work, the following conclusions can be drawn:

- A hard layer consisting of a biphasic FeB/Fe_2B-type layer can be formed to enhance the surface properties of AISI 304L steel via a thermochemical process called powder-pack boriding.
- The boride layer formed on AISI 304L steel tends to become thicker and tougher as treatment time increases.
- Unlike the boride layers formed on low-alloy and low-carbon steels, the boride layer formed on AISI 304L steel is a biphasic layer composed mainly of FeB/Fe_2B. This is probably a consequence of the high concentration of alloy elements in the studied steel, which act as a diffusion barrier, forcing an increase in the boron flow to the surface and, therefore, its concentration, which is enough to form the FeB phase.
- The cellular viability assays indicated a high percentage of living HFOb cells in the samples exposed to 2 h of the boriding process in the first 24 h of culture (step 1). However, after the next 24 h (step 2), the samples exposed to 4 h of treatment showed the highest concentration of living HFOb cells, indicating the best treatment condition for possible biomedical applications.
- Compared with the literature's report on AISI 316L steel exposed to the boriding process, no significant differences were observed in the resulting layers in this research, indicating that molybdenum does not influence the formation of boride layers.

ACKNOWLEDGMENTS

This research was funded by the Instituto Politécnico Nacional, México, grant number SIP20240924.

The authors thank the National School of Medicine and Homeopathy of the Instituto Politécnico Nacional for its invaluable contribution to this work. Additionally, they thank the Universidad Autónoma de Coahuila and the Universidad de las Américas Puebla in México for their collaboration in developing this work.

REFERENCES

1. Gurpreest Singh, Hazoor Singh, Buta Singh Sidhu, 2013, "Corrosion behavior of plasma sprayed hydroxyapatite-silicon oxide coating on AISI 304 for biomedical application", Applied Surface Science, vol. 284, pp 811-818.
2. I. Ozbek, B. A. Konduk, C. Bindal, and A. H. Ucisik, 2002, "Characterization of borided AISI 316L stainless steel implant," Vacuum, vol. 65, no. 3-4, pp. 521–525.
3. Duan, Y.; Wang, X.; Liu, D.; Bao, W.; Li, P.; Peng, M., 2020 "Characteristics, wear and corrosion properties of borided pure titanium by pack boriding near α → β phase transition temperature". Ceramics International, vol. 46, no. 10, Part B, pp 16380–16387.
4. Himanshu Balhara, Cagatay Yelkarashi, Ali Erdemir, Satish T.S. Bukkapatnam, 2024, "Spatial characteritics of ultra hard coating on direct energy deposition (DED)-printed 316L with a novel ultra-fast boriding", Journal of Manufacturing Process, vol. 121, pp 92-99.
5. M.Y. García_Santibañez, J.G. Quiñonez-Galvan, N. López Perrusquia, M. A. Doñu Ruiz, E. García, 2023, "Study of wear, process, generated by cavitation phenomena produced by laserd induced dielectric breakdown on borided and non-borided 316L stainless steel surface in bi-distilled water", Materials Letters, vol. 343.
6. R.A. García-León. J. Martínez-Trinidad, M. Palomar-Pardavé, L. Lartundo-Rojas. A. Guevara-Morales, H. Martínez-Gutiérrez, 2024, "Tribomechanical products on borided AISI 316L Steel exposed to Hank´s solution", Wear, vol. 538-539, pp. 1-15.
7. Ravi Kumar, Anil Kumar Das, Ma, 2024, "A comprehensive review of AISI 304 steel based on different thick coating process", Materials Today: Proceedings, vol. 98, pp. 180-186.
8. Alexis Chino-Ulloa, Mario Hernandes-Alejandro, José L. Castrejón-Flores, Moisés Cabrera-González, Itzel P. Torres-Avila, Julio C. Velázquez, Pablo A. Ruiz-Trabolsi and Enrique Hernández-Sánchez, 2029, "Development of Ultra-Low Friction Coefficient Films and Their Effect on the Biocompatibility of Biomedical Steel", Materials Transactions, vol. 60, no.8, pp. 1605-1613.
9. E. Hernández-Sánchez, A. Chino-Ulloa, J. C. Velazquez, H. Herrera-Hernández, R. Velázquez-Mancilla, and R. Carrera-Espinoza, 2015, "Effect of Relative Humidity on the Tribological Properties of Self-Lubricating H3BO3 Films Formed on the Surface of Steel Suitable for Biomedical Applications", Advances in Materials Science and Engineering, vol. 2015, pp. 1-9.
10. Türkmen I.; Yalamaç E., 2018, "Growth of the Fe_2B layer on SAE 1020 steel employed a boron source of H3BO3 during the powder-pack boriding method". Journal of Alloys and Compounds, vol. 744, 558–666.
11. Campos I.; Oseguera J.; Figueroa U.; García J.A.; Bautista, O.; Kelemenis G., 2023, "Kinetic study of boron diffusion in the paste boriding process". Materials Science and Engineering A, vol. 352, pp. 261–265.
12. Ouyang, D.; Cui, X.; Lu, S., 2021, "Growth kinetics of the FeB/Fe_2B boride layer on the surface of 4Cr5MoSiV1 steel Experiments and modelling", Journal of Materials Research and Technology, vol. 11, pp. 1272–1280.

13. ASTM E-384-05a; Standard Test Method for Microindentation Hardness of Materials. The American National Standards Institute: Washington, DC, USA, 2005.
14. Ávila Portillo, Luz Mabel, Madero, José I, López, Claudia, León, María Fernanda, Acosta, Lucía, Gómez, Claudia, Delgado, Lucy Gabriela, & Gómez, Claudio., 2006. "Fundamentos de Criopreservación", Revista Colombiana de Obstetricia y Ginecología, vol. 57, no. 4, pp. 291-300. Retrieved july 27, 2024, from: http://www.scielo.org.co/scielo.php?script=sci_arttext&pid=S0034743420060004000008&lng=en&tlng=es
15. Saenz Muñoz B. 2021, "Evaluación del metabolismo de la resazurina en función de la forma y tamaño de esferoides tumorales orales", [tesis de pregrado], p 9, pp. 1-44, Universidad del bosque, Bogotá Colombia.
16. A. Graf von Matuschka: Boronizing, 1st ed., (Carl Hanser, Munich, Germany, 1980).
17. M. Carbucicchio and G. Palombarini, 1987, "Effect of alloying elements on the growth of iron boride coatings", Journal of Materials Science Letters, vol. 6, pp. 1147-1149.
18. I. Campos-Silva, M. Ortiz-Domínguez, O. Bravo-Bárcenas, M.A. Doñu-Ruiz, D. Bravo-Bárcenas, C. Tapia-Quintero and M.Y. Jiménez-Reyes, 2010, "Formation and kinetics of FeB/Fe2B layers and diffusion zone at the surface of AISI 316 borided steels, Surface and Coatings Technology. vol. 205, pp. 403-412.
19. O. Ozdemir, M.A. Omar, M. Usta, S. Zeytin, C. Bindal and A.H. Ucisik, 2008, "An investigation on boriding kinetics of AISI 316 stainless steel", Vacuum, vol. 83, no. 1, pp. 175-179.
20. Ouyang, D.; Cui, X.; Lu, S., 2021, "Growth kinetics of the FeB/Fe_2B boride layer on the surface of 4Cr5MoSiV1 steel: Experiments and modelling", Journal of Materials Research and Technology, vol.11, pp. 1272–1280.
21. Kulka, M.; Makuch, N.; Dziarski, P.; Piasecki, A. 2014, "A Study of Nanoindentation for Mechanical Characterization of Chromium and Nickel Borides' Mixtures Formed by Laser Boriding", Ceramics International, vol. 40, pp. 6083–6094.
22. Türkmen, I.; Yalamaç, E., 2018, "Growth of the Fe2B layer on SAE 1020 steel employed a boron source of H_3BO_3 during the powder-pack boriding method", Journal of Alloys and Compounds., vol. 744, 558–666.
23. Martínez-Nopala, S.R.; Figueroa-Lopez, U.; Guevara-Morales, A.; Campos-Silva, I., 2024, "Solid particle erosion resistance of borided AISI D2 Steel". Materials Today Communications. Vol. 38, 107887
24. Zhang, D.; Li, Y.; Du, X.; Fan, H.; Gao, F., 2022 "Microstructure and Tribological Performance of Boride Layers on Ductile Cast Iron under Dry Sliding Conditions", Engineering Failure Analysis, vol. 134.
25. Milinovi´c, A.; Maruši´c, V.; Konjati´c, P.; Beri´c, N., 2022, "Effect of Carbon Content and Boronizing Parameters on Growth Kinetics of Boride Layers Obtained on Carbon Steels", Materials, vol. 15, 1858., pp. i-17.
26. Enrique Hernández-Sánchez, Diego Hernández-Domínguez, Raúl Tadeo-Rosas, Yesenia Sánchez-Fuentes, Luz Alejandra Linares-Duarte, Carlos Orozco-Álvarez, José Guadalupe Miranda-Hernández and Rafael Carrera-Espinoza, 2024, "Tribological and Mechanical Behavior of Automotive Crankshaft Steel Superficially Modified Using the Boriding Hardening Process", coatings, vol. 14, no.716, pp. 1-14.
27. G.A. Rodríguez-Castro, R.C. Vega-Morón, A. Meneses-Amador, H.W. Jiménez-Díaz, J.A. Andraca-Adame, I.E. Campos-Silva, M.E. Palomar Pardavé, 2016, "Multi-pass scratch test behavior of AISI 316L borided Steel", Surfaces and Coatings Technology, vol. 307, pp. 491–499.

28. I. Ozbek, B.A. Konduk, C. Bindal, A.H. Ucisik, 2022, "Characterization of borided AISI 316L stainless steel implant", Vacum, vol. 65, no. 3-4, 521–525.
29. R.A. García-León, J. Martínez-Trinidad, I. Campos-Silva, U. Figueroa-López, A. Guevara-Morales, 2021, "Development of tribological maps on borided AISI 316L stainless Steel under ball-on-flat wet sliding conditions", Tribology international, vol. 163, pp. 1-14.
30. Hernández Sánchez, E. Propiedades Mecánicas de Aceros Borurados AISI 1018 Evaluadas por Indentación a Escala Micro y Nanométrica; Instituto Politecnico Nacional: Mexico City, Mexico, 2011.